Progress in Physics of Applied Materials 5 (2025), Serial Number 9, 137– 150

Semnan University

Progress in Physics of Applied Materials

journal homepage: https://ppam.semnan.ac.ir/

Study of Synthesis Dependent Physicochemical and Optoelectronic Properties of Nanocrystalline Lead Sulfide (PbS) Thin Films Deposited using Chemical Bath Deposition Method

Narayani Madhukar Gosavi [a], Kunal Rajabhau Sali [a], Rajesh Arun Joshi [b*], Sunil Rameshgir Gosavi [a*]

[a] *Material Research Laboratory, C.H.C. Arts, S.G.P. Commerce and B.B.J.P. Science College, Taloda, Dist. Nandurbar, MS, India 425413*

[b] *Thin Film and Sensor Laboratory, Department of Physics, Toshniwal Arts, Commerce and Science College, Sengaon Dist. Hingoli MS India 431542*

ARTICLE INFO

Article history:
Received: 28 February 2025
Revised: 17 April 2025
Accepted: 20 April 2025
Published online: 17 Jun 2025

Keywords:
Sensor;
PbS;
Thin Films;
Optoelectronic Properties;
Chemical Bath Deposition.

ABSTRACT

The present paper deals with the synthesis of PbS thin films using cost cost-effective chemical route over the glass substrates at room temperature for studying the effect of deposition time on physicochemical and optoelectronic properties with the intension to test the application as an ammonia gas sensor. These 10, 20, 30, 40, and 50 min deposited thin films have been characterized for their structural properties using X-ray diffraction patterns (XRD), which revealed stoichiometric PbS thin films having a polycrystalline cubic structure with orientation along the (111) and (002) planes, with crystallite sizes varying from 18 to 22 nm. The Raman spectrum shows peaks at 92 and 143 cm-1, representing the transverse and longitudinal oscillations for chemical ionic bonds, respectively. The elemental analysis confirmed from the energy dispersive X-ray analysis spectrum infers expected and observed chemical compositions in PbS thin films. The surface topography and morphology have shown the floral distribution of grains over the substrate surface. This exhibited the effect of deposition time in the form of flower growth. PbS synthesized for 40 min represents a completely grown flower, while dipping time less than 40 min shows a slightly varying nature of the flower. Such topography could be useful for surface-related applications. The optical absorbance spectra represented the higher absorbance coefficient and energy band gap calculated to be 1.48 eV, which inferes the polaron-induced charge transfer. The ammonia gas sensitivity calculated as a function of optical absorbance in air and under gas impurging has shown at most 80% sensitivity for the thin film grown by dipping 40min in the precursor solutions.

1. Introduction

Metal chalcogenide nanostructures have received increasing attention of researchers owing to its potential physical and chemical properties which might have been resulted due to precise aspect ratio of the materials. Amongst various metal chalcogenide semiconductor combinations lead sulfide (PbS) nanostructure exhibited the dynamic nature for applications into optoelectronic device such as luminescent devices, photochemical cell, solar cell, diode laser, photodetectors, efficient heterojunction photovoltaic cell, gas sensors etc. [1-4]. PbS has occupied distinguished position among materials from IV-VI binary semiconductor due to its properties like small band gap, abundance in nature, relatively large exciton Bohr radius of 18 nm and high chemical stability [5].

Owing to the smaller band gap, PbS possesses special optoelectronic properties and has larger range of applications as optoelectronic gadgets, detectors, etc. [6]. Such kind of materials are highly preferred in areas like

* Corresponding author. Tel.: +91-7775058884, +91-9881625833
E-mail address: urajoshi@gmail.com, srgosavi.taloda@gmail.com

Cite this article as:
Gosavi N.M., Sali K.R., Joshi R.A., and Gosavi R.S., 2025. Study of Synthesis Dependent Physicochemical and Optoelectronic Properties of Nanocrystalline Lead Sulfide (PbS) Thin Films Deposited using Chemical Bath Deposition Method. *Progress in Physics of Applied Materials*, *5*(2), pp.137-150. DOI: **10.22075/PPAM.2025.37005.1134**

photography, sensors, and solar absorbers. Additionally, PbS also used as photo-resistance, LASER, humidity, and temperature sensors. In comparison to bulk, the thin film results in good photovoltaic properties. PbS thin film is one of the prominent materials used to detect hazardous gases like ammonia, H2S, NO2, etc. [7].

Also, efficient light-absorbing capacity in the visible to near-infrared range, relatively longer life exciton time, makes PbS suitable for the fabrication of thin film-based sensors [8].

Meanwhile, in last few decades, many researchers undertook significant contribution for fabricating good quality nanocrystalline PbS thin films using several deposition techniques such as molecular beam epitaxy (MBE) [9], RF-sputtering deposition method [7, 10], glancing angle deposition (GLAD), physical vapor deposition (PVD) [11], vacuum thermal evaporation [12], chemical vapor deposition [13], electrodeposition [14, 15], spin coating [16], spray pyrolysis [17, 18], liquid flow deposition [19], microwave-assisted chemical bath deposition [20], SILAR [21-22], and chemical bath deposition (CBD) [23]. Among these deposition techniques, CBD method is one of the widely used and inexpensive techniques and it has shown advantages of low temperature synthesis, well suited for large area deposition, reproducibility, it does not require any sophisticated equipment and most important is its compatibility with other synthesis methods. It is possible to control the film thickness by varying the parameters such as pH, precursor concentration, and deposition time and temperature, etc., thus increasing the absorption capability useful for sensor development. The morphological and structural characteristic of chemically deposited PbS films may affect their electrical and optical properties. While the features of electrical transport in PbS films are those characteristics of materials constituted by grains and grain boundaries, hence surface roughness and voids in the films strongly affect their optical spectra.

The literature survey revealed that the film synthesis time i.e. deposition time majorly affect the optoelectronic properties but very few reports are available about PbS thin film deposition at varying dipping time. Hence, consider the significance of this, in the present paper we deal with PbS thin films synthesis at different time intervals and study its effect on potential properties with vision to use it as surface-based gas sensing material [24-26]. As such deposited thin films characterized for structural, compositional, morphological, optical and electrical properties as well as NH_3 gas sensing characteristics respectively.

2. Experimental Details

All paragraphs should be indented and justified in alignment. The font of the entire document should be Cambria.

2.1. Substrate Cleaning

The nanocrystalline PbS thin films synthesized using low cost and simple chemical bath deposition method over glass substrates at room temperature. The glass slides of the dimension 7.3 x 2.5 x 0.1 cm^3 procured from blue-star Company have been used as the substrates. In solution growth technique**,** extreme cleanliness of the substrate is required, since the contaminated surface provides nucleation sites facilitating the growth, and resulting into non-uniform, porous, and non-adherent film. The following procedure has been used for cleaning of the substrates.

a) The slides were washed with water.
b) Then boiled in concentrated chromic acid (0.5M) for 1h and kept in it for 24h.
c) The boiled substrates were washed with double distilled water, and
d) Finally, the substrates were dried, degreased in AR grade acetone and were kept in dust free airtight container.

2.2. Solution Preparation

The chemical ingredients used for nanocrystalline PbS thin films synthesis using chemical bath deposition method over glass substrates at room temperature are as followings:

1. 0.1M solution of $(CH_3COO)2Pb.3H_2O$ as a source of Pb^{2+} ions
2. 0.1M solution of $(NH_2)_2CS$ as a source of S^{2-} ions
3. 25% Ammonia [NH_4OH]

The 0.1M solution of $(CH_3COO)_2Pb._3H_2O$ as a source of Pb^{2+} ions, $(NH_2)_2CS$ as a source of S^{2-} ions while, Triethanolamine ($C_6H_{15}NO_3$) (TEA) used as complexing agent to prevent the metal oxide formation, and 25% Ammonia [NH_4OH] used for adjusting the pH of the reaction mixture. These chemicals used here are AR grade purchased from LOBA Chemie, Pvt. Ltd. Mumbai India. All the solutions were prepared in fresh double distilled water.

2.3. PbS Thin Film Synthesis

The nanocrystalline PbS thin films synthesized using chemical bath deposition method over glass substrates with dipping time intervals of 10min, 20min, 30min, 40min, and 50min. The nanocrystalline PbS thin films were prepared from aqueous alkaline bath using 0.1M solution of $(CH_3COO)_2Pb._3H_2O$, 0.1M solution of $(NH_2)_2CS$, and ammonia [27, 28].

For the synthesis of nanocrystalline PbS thin films, the chemical bath contains 20 ml of 0.1M solution of $(CH_3COO)_2Pb._3H_2O$ in which few drops of 25% ammonia slowly added for complex formation under constant stirring. Subsequently, 20 ml of 0.1M solution of $(NH_2)_2CS$ was added into this mixture and stirred well for few minutes. The pH of the bath was adjusted to a suitable value at which ionic product exceeds the solubility product (pH≈9). Then, this reaction mixture of dark brownish color was transferred into a 50 ml beaker, in which the well cleaned glass substrates were kept vertically using the substrate holder. The deposition was allowed to proceed with continuous stirring the solution and carried out at constant temperature (50^oC). The substrates coated with PbS film were removed from the bath at suitable intervals (10 min, 20 min, 30 min, 40 min, 50 min), washed with deionized water, dried in air and preserved in a container. As such obtained thin films of PbS were maintained in dark desiccator for prevention against additions of any other impurity over the materials surface.

Such a chemically grown nanocrystalline PbS thin films characterized for structural characteristics using X-ray diffraction method conducted using the D8 Advanced Diffractometer, while compotional analysis conducted using energy dispersive X-ray analyais (EDAX) spectra counted with the help of FEI made Nova Nanosem 450 Fe-Sem Rv along with surface morphology using field emission scanning electron microscopy (FESEM), Raman spectra recorded using Horiba Jobin-Yvon HR 800, Japan while absorbance spectra counted over UV-visible light spectrometer JASCO V-630 model, and resistivity measurement was conducted using lab made Kiethley I-V set up.

2.4. Thin Film Synthesis Mechanism

The deposition of nanocrystalline PbS thin films onto the cleaned glass substrates by CBD was done using lead acetate-ammonia-thiourea system that consists of complexation of the Pb^{2+} cations by the ammonia and thereby consecutive reaction with the S^{2-} ions provided through the hydrolysis of thiourea.

The overall reaction of formation of PbS can be written as follows,

$$[Pb(NH_3)_4]^{2+}{}_{aq} + CS(NH_2)_{2\,aq} + 2OH^-{}_{aq} \rightarrow PbS_s + 4NH_{3\,(l)} + CH_2N_{2\,(aq.)} + 2H_2O_{(l)}$$

Fig. 1. Change in color of the observed PbS thin films at different intervals of dipping time (a) 10 min, (b) 20 min, (c) 30 min, (d) 40 min, (e) 50 min

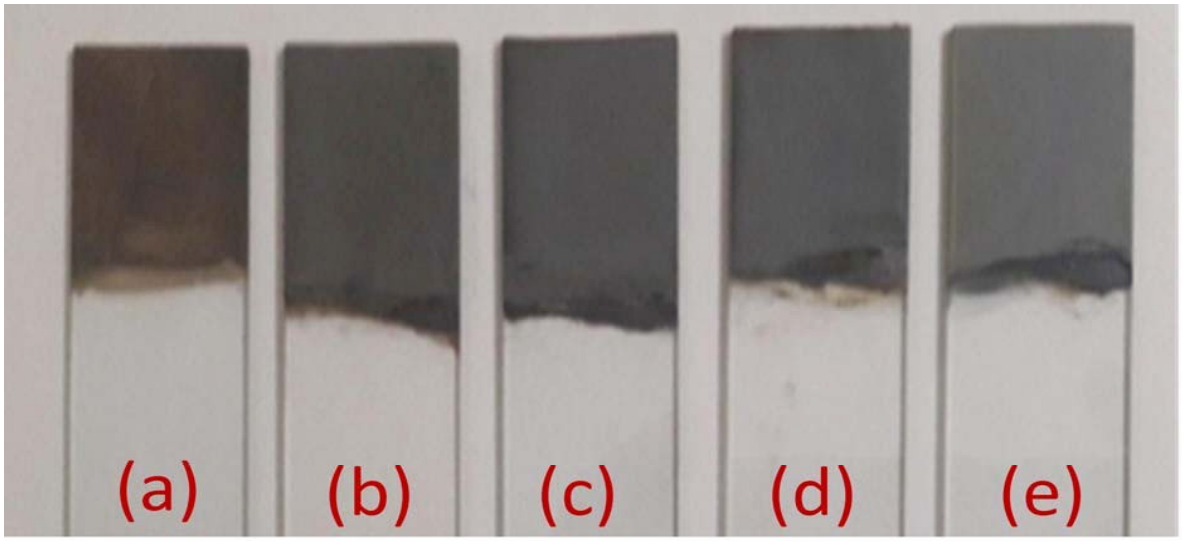

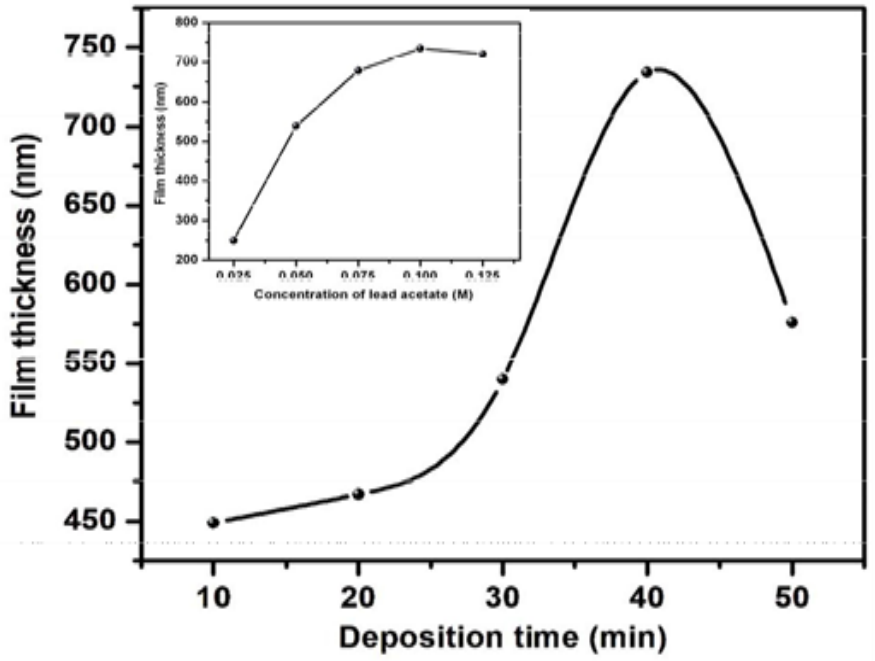

Fig. 2. Plot of deposition time against film thickness while inset image shows Pb^{2+} ion concentration against film thickness.

Fig. 1 shows the variation of PbS film color for various concentrations of lead acetate for thiourea (source of S^{2-} ions).

During deposition process, it was observed that film thickness increased with lead acetate concentration and reached maximum value (≈734 nm) at 0.1 M, then it films thickness decreased, since formation of outer porous layer leads to decreasing film thickness. Growth mechanism of nanocrystalline PbS thin film deposited by CBD based on the controlled precipitation of PbS in chemical bath. Here, ammonia is used to control free lead ions (Pb^{2+}) concentration, complex is formed by Pb^{2+}, ammonia and hydroxide which react with thiourea to form PbS from adsorbed metastable complex. Fig. 2 shows thickness of the nanocrystalline PbS thin film as a function of deposition time. From this figure we found that, during deposition process, film thickness tends to increase with time (till 40 min), thereafter it starts slight decrease may be due to excess ion stabilizes the complex ions and reduces growth rate [29]. This decrease in film thickness can be seen from the plot of thickness variation as a function of deposition time (see Fig. 2).

3. Results and Discussion

3.1. Structural Analysis

Fig. 3 represents X-ray diffraction (XRD) obtained for the PbS thin films deposited at different time intervals (deposition time or dipping time of substrate) showing influence of deposition time on crystalline state of deposited films. Comparing XRD patterns of the deposited films with JCPDS card no 78-1901, it is confirmed that PbS thin films exhibit face centered cubic structure with (111) and (002) planes as preferred orientations. For films deposited with 20 min duration, the most intense reflection occurs along (002) plane at 2θ ≈ 29.71°. The intensity of (111) reflection appears relatively less in comparison to (002). In addition to (002) and (111) reflections, other minor reflections are also clearly seen along (220) and (311) planes at 2θ ≈ 42.76° and 50.67°, respectively [30-32]. This indicates the formation of polycrystalline cubic structure for all samples. Crystallographic properties of the nanocrystalline PbS thin films deposited with different deposition times are summarized in Table 1.

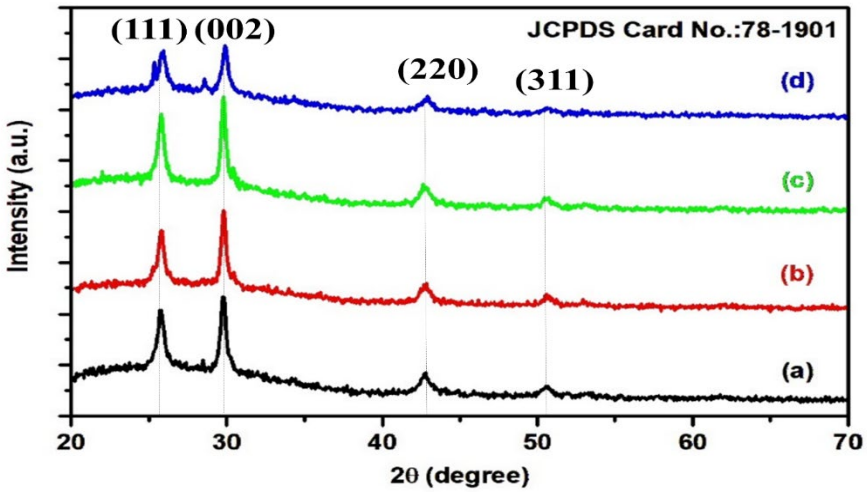

Fig. 3. X-ray diffraction (XRD) pattern of PbS thin film for different synthesis time represented by (a) 20 min, (b) 30 min, (c) 40 min, and (d) 50 min

Table 1. Experimental XRD data of nanocrystalline PbS films prepared at different deposition times

JCPDS (78-1901)			Experimental XRD data							
			20 min.		30 min.		40 min.		50 min.	
Peaks (h k l)	2θ (deg.)	d (Å)	2θ (deg.)	d (Å)	2θ (deg.)	d (Å)	2θ (deg.)	d (Å)	2θ (deg.)	d (Å)
(1 1 1)	25.998	3.4245	25.68	3.4664	25.83	3.4462	25.83	3.4463	25.99	3.4249
(2 0 0)	30.108	2.9657	29.71	3.0041	29.71	3.0045	29.87	2.9889	30.03	2.9728
(2 2 0)	43.10	2.0971	42.76	2.1126	42.76	2.1126	42.6	2.1207	42.9	2.1062
(3 1 1)	51.026	1.7884	50.67	1.8001	50.52	1.8051	50.67	1.8001	50.67	1.8001

However, for PbS films deposited with deposition time of 50 min, additional peak is observed at 2θ ≈ 28.60°, this might be attributed due to the presence of impurity (PbO). Table 1 shows the value of interplanar spacing (d) which was calculated by using the Bragg's equation $2d_{hkl} \sin\theta = n\lambda$, where d_{hkl} is lattice spacing of hkl plane, θ is the Bragg angle, n is the order of diffraction (usually n = 1 for first order), λ is the X-ray wavelength, and h, k, and l are the Miller indices. The obtained d values are in good agreement with those mentioned in the standard JCPDS data.

As a result of increase in deposition time, the increase in the intensity of the peaks were observed up to deposition time of 40 min, while for film deposited for 50 min, reflects variation in intensity and dissimilation of peaks, may be

due to decrease in film thickness. The PbS films prepared with deposition time of 20 min has average crystallite size of ~ 18.04 nm, while for further higher deposition times, the crystallite size increases significantly. We herewith found that, the crystallite size increases from 18.04 to 22.20 nm as deposition time increases from 10 to 40 minute and again it decreases to 16.03 nm for higher deposition time of 50min as calcualted from the Debye Scherrer formula.

$$D = \frac{k\lambda}{\beta Cos\theta} \quad (1)$$

Where D is the crsytallite size, k is a constant (often 0.94), λ is the X-ray wavelength, β is the full width at half maximum (FWHM) of the diffraction peak, and θ is the Bragg diffraction angle.

This shows that the crystalline quality of the deposited PbS thin films varies with the deposition time. The increase in crystallite size with deposition time may be attributed to the favorable variation in the film thickness and more number of particles attarcted towards the substrate. While at higher deposition time (50 min), the decrease in crystallite size of the films is attributed to the peeling of the films, due to the formation of outer porous layer or the films may have developed stress which tends to cause delamination [33]. Further, the number of defects in synthesized thin films, dislocation density (δ) and average microstrain ($\boldsymbol{\varepsilon}$) developed in the prepared thin films, and lattice parameter (a) calculated and tabulated in table 2 using the William Hall equations and plotting.

Table 2. Structural parameters of nanocrystalline PbS films prepared at different deposition times

Deposition time (Min)	Film thickness (nm)	Average Crystallite size (D) (nm)	Lattice parameter (a) (Å)		Micro-strain $\varepsilon \times 10^{-3}$	Dislocation density $\rho \times 10^{15}$ Lines/m^2	Number of crystallites per unit area ($N \times 10^{16}$)
			JCPDS	Observed			
20	467	18.04	5.9315	5.9894	2.1589	4.2627	7.95
30	540	21.61		5.9850	1.9043	3.5264	5.35
40	734	22.20		5.9789	1.8470	3.2334	6.71
50	576	16.03		5.9513	2.4250	5.3177	13.98

$$\beta Cos\theta = 4\varepsilon Sin\theta + \frac{k\lambda}{D} \quad (2)$$

Where D is the crsytallite size, k is a constant (often 0.94), λ is the X-ray wavelength, β is the full width at half maximum (FWHM) of the diffraction peak, ε is lattice strain, and θ is the Bragg diffraction angle.

The calculated value of the lattice parameters showed a slight deviation from its standard value and these values were fluctuated slightly with the deposition time which can inferred as strain [34].

3.2. Raman Spectroscopy

The Raman spectra for the nanocrystalline PbS thin films prepared with deposition time of 20, 30, 40, and 50 min are shown in Fig. 4.

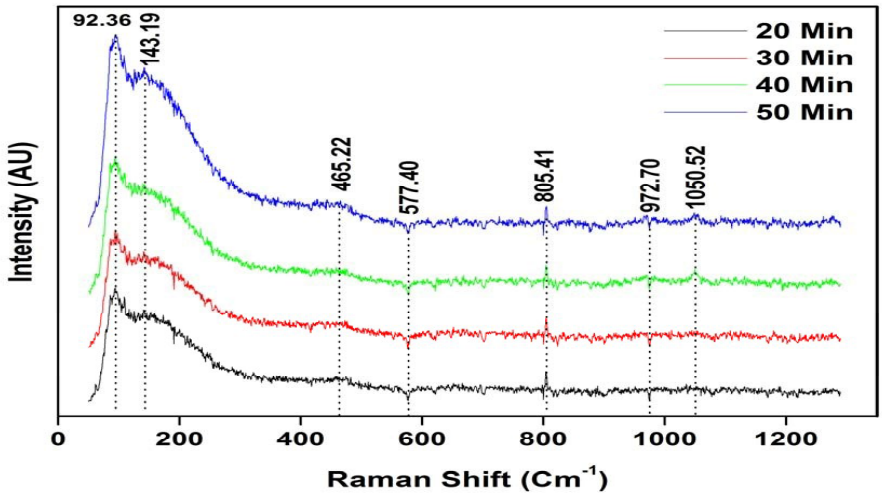

Fig. 4. Raman spectra for nanocrystalline PbS thin films deposited at time intervals of 20, 30, 40, and 50 min

This figure indicates the presence of two major vibrational active and five minor modes, and no significant shift in peak position was observed. Peak at approximately 92 cm^{-1} might be attributed to a combination of longitudinal and transverse acoustic (LA+TA) phonon modes in PbS thin films [35]. The less intensity second peak at 143.19 cm^{-1} might be originated from a combination of transverse acoustic and transverse optical (TA+TO) phonon modes [35]. Thus, this study confirms the prepared sample consists of pure PbS without the presence of sulphates and other impurities. All Raman modes are seen at low wavenumber positions, when compared with bulk

PbS owing to small size, used laser, and direction of growth of PbS nanoparticles over the substrate surface. Although no major changes in the peak positions are observed but slight variations in the intensity and growing of neck kink around the larger peak 143cm^{-1} can be observed in the thin films synthesized at 40 and 50min durations, which can be correlated to saturation level of PbS synthesis.

3.3. Compositional Analysis

Fig. 5 represents the elemental compositional analysis of the PbS thin films conducted using the energy dispersive X-ray analysis spectra which infers the elemental proportion as expected and used for the film synthesis.

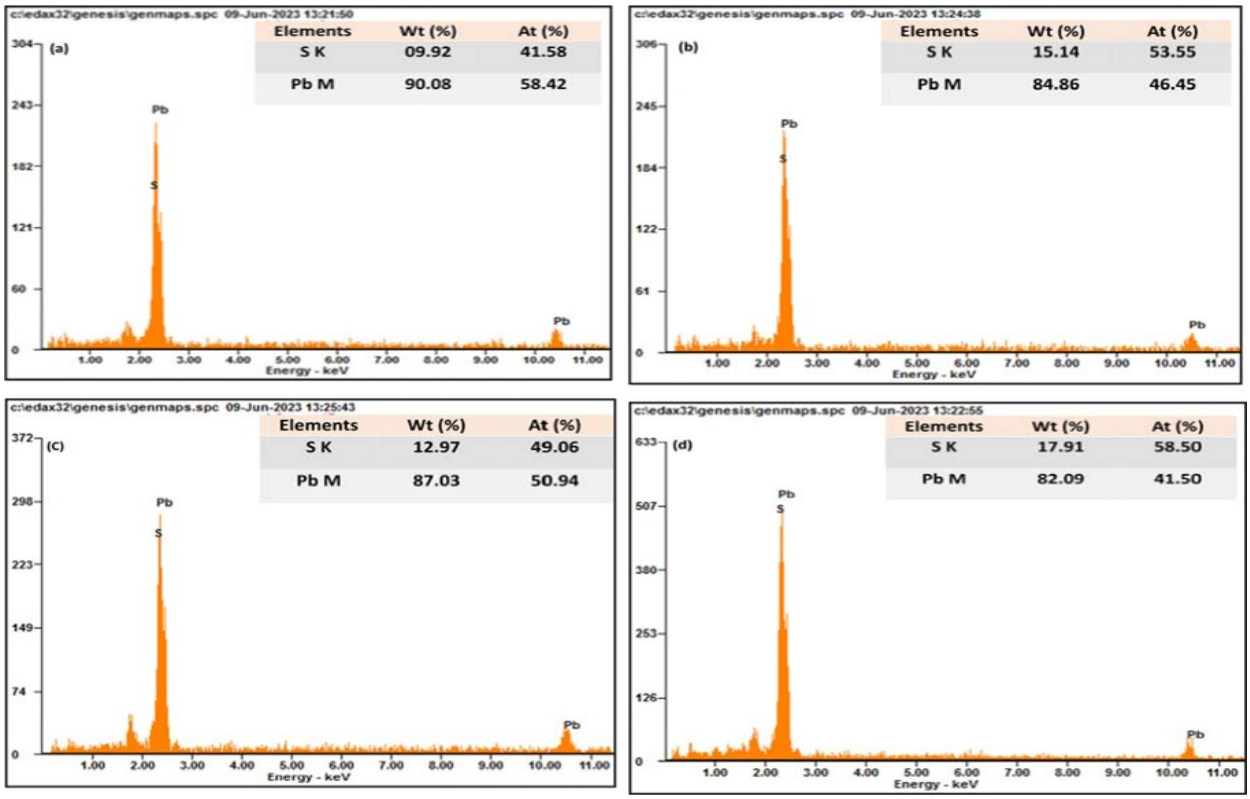

Fig. 5. EDAX spectra for PbS films deposited at (a) 20 min, (b) 30 min, (c) 40 min, and (d) 50 min

Table in the inset of the figures shows that the element proportion for the film deposited at 40 min is nearly equal, while films deposited at 20 and 30 min represent the lower contribution of the elements.

The analysis confirms the presence of the Pb and S elements in the deposited films. It is noted that some additional peaks are also observed which might be attributed due to the amorphous glass substrates.

It is also found that the deposition time affect the Pb/S atomic ratio as represented in Table 3. However, perfect stoichiometric PbS film formed when the deposition time is 40 minutes.

Table 3. Atomic compositions of the nanocrystalline PbS thin films deposited at different deposition times.

Deposition time (min)	Element	Series	Atomic %	Pb/S atomic ratio
20	S	K	58.97	0.70
	Pb	M	41.03	
30	S	K	41.58	1.40
	Pb	M	58.42	
40	S	K	49.06	1.04
	Pb	M	50.94	
50	S	K	53.55	0.87
	Pb	M	46.45	

3.4. Surface Morphology

Fig.6 illustrates the field emission scanning electron microscopy (FESEM) images of 40 min dipping time PbS thin films. Low resolution image shows that high density flower-like PbS architectures uniformly grow and highly disperse over the substrate surface without any aggregation.

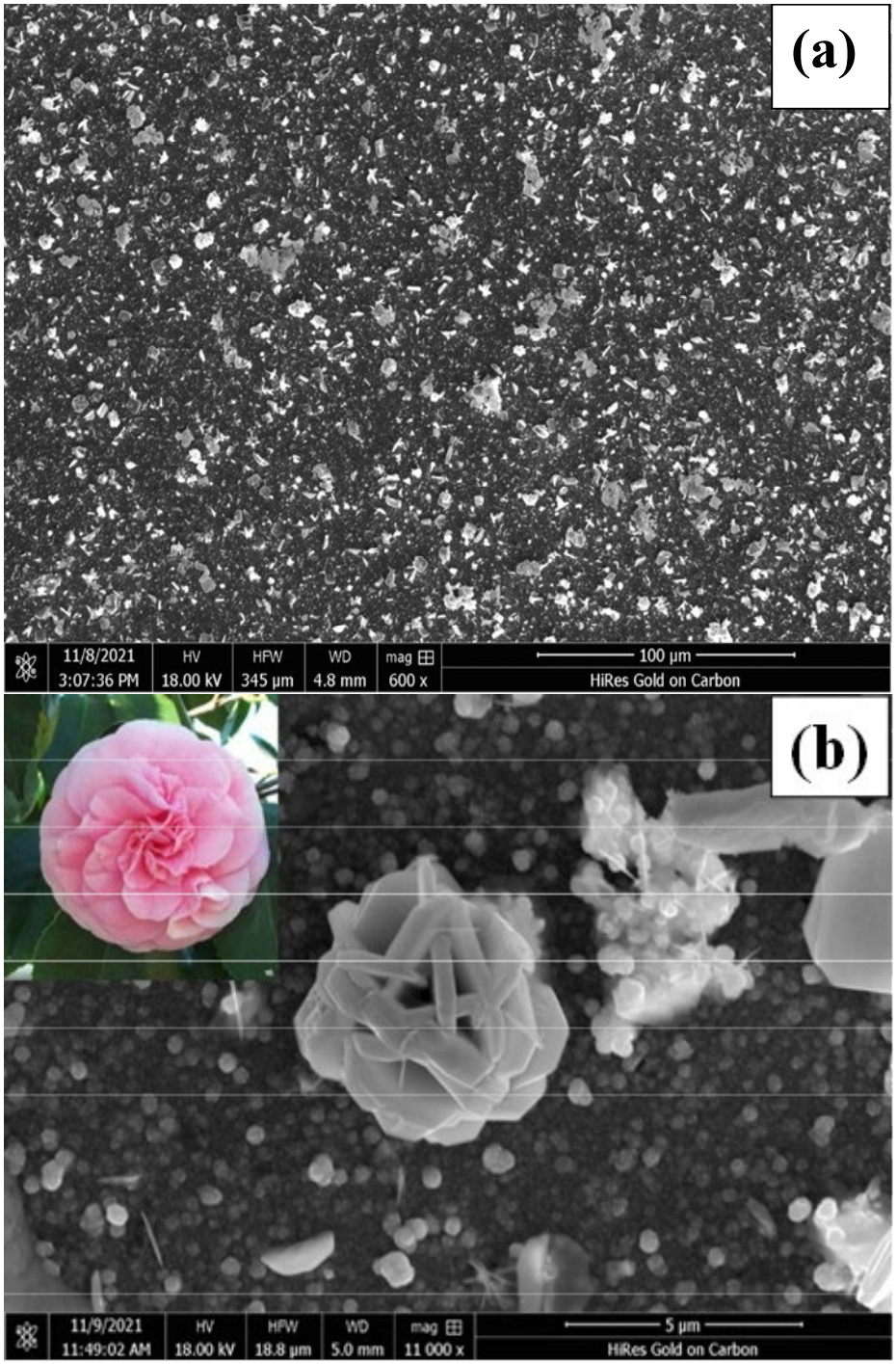

Fig. 6. FESEM micrographs of flower-like PbS nanostructure prepared by CBD deposited at 40 min (a) Low resolution images, (b) isolated PbS flower (Inset shows photographs of natural camellia flower)

The magnified FESEM image clearly revealed that chemically synthesized PbS exhibits well-defined flower-like morphology in their geometrical features. It also shows that each flower has a diameter of about 4-5 µm in length, 1.5-2 µm in width, and about 500 nm in thickness, which are assembled to form the flower-like PbS architectures and consists of 20-25 thin nanosheets which are projected from the surface of the substrate. To investigate the detailed growth process of the flower-like PbS nanostructures, we have carried out the time-dependent chemical reaction in the bath at 50^{o}C under the normal pH condition. The evolution of morphology in the film formation process has also been investigated and FESEM images (Fig 7 (a), (b), (c), and (d)) shows slightly different

structurally evolved stages of the film formation process obtained at different deposition times.

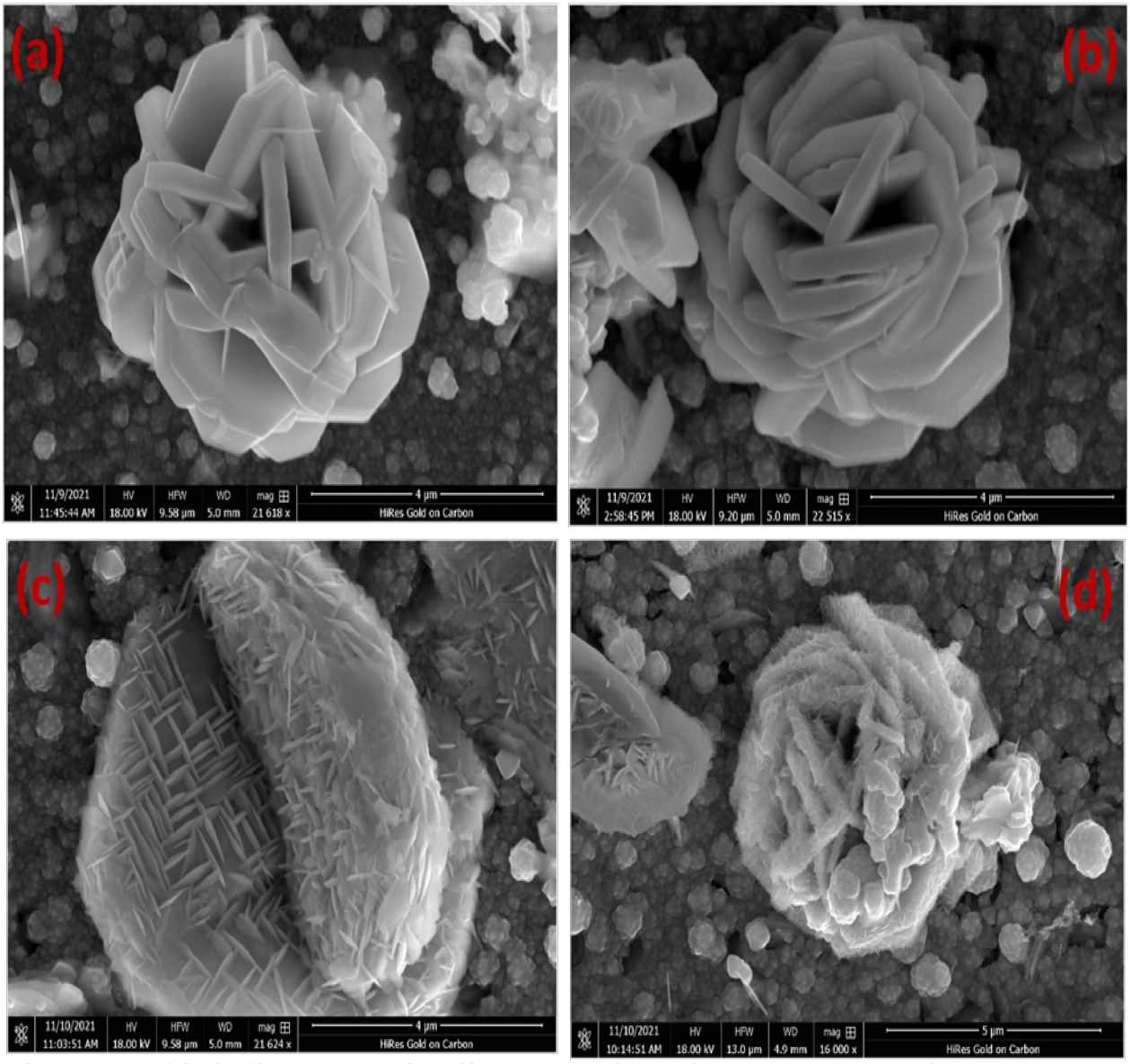

Fig. 7. The SEM images of PbS thin films representing flower like structures for different deposition times (a) 20 min, (b) 30 min, (c) 40 min, and (d) 50 min

Hence it can be claimed that CBD method is very useful for formation of PbS nanostructures with nanoflower-like and nanosheet-like morphology. Metal sulfides nanostructures with such kind of morphology are very helpful in using the materials for surface-based properties like gas sensing, photovoltaic cell, next-generation high performance energy storage device applications, etc. [11].

The surface morphology of chemically synthesized nanocrystalline PbS thin films deposited by varying the deposition time has also been studied by using atomic force microscopy (AFM) as shown in Figs. 8 (a), (b), (c), and (d) for dipping times of 20, 30, 40, and 50 min respectively. From the above figures it can be seen that the substrate surface is well covered with the grains that are uniformly and regularly distributed over the surface, indicating the formation of more nucleation sites. It can be observed that by increasing the deposition time the grain size and surface roughness changes [34, 35]. Table 4 tabulates the grain size and root mean square (RMS) roughness of the different nanocrystalline PbS thin films. Topographic images of the films depict that the higher deposition time leads to bigger grains at the surface which are in good agreement with the XRD results. Such behavior indicates that the film growth proceeds through agglomeration of the islands with increasing of deposition time [36]. The (RMS) roughness value increases with deposition time and it is found to be in the range 104-256 nm.

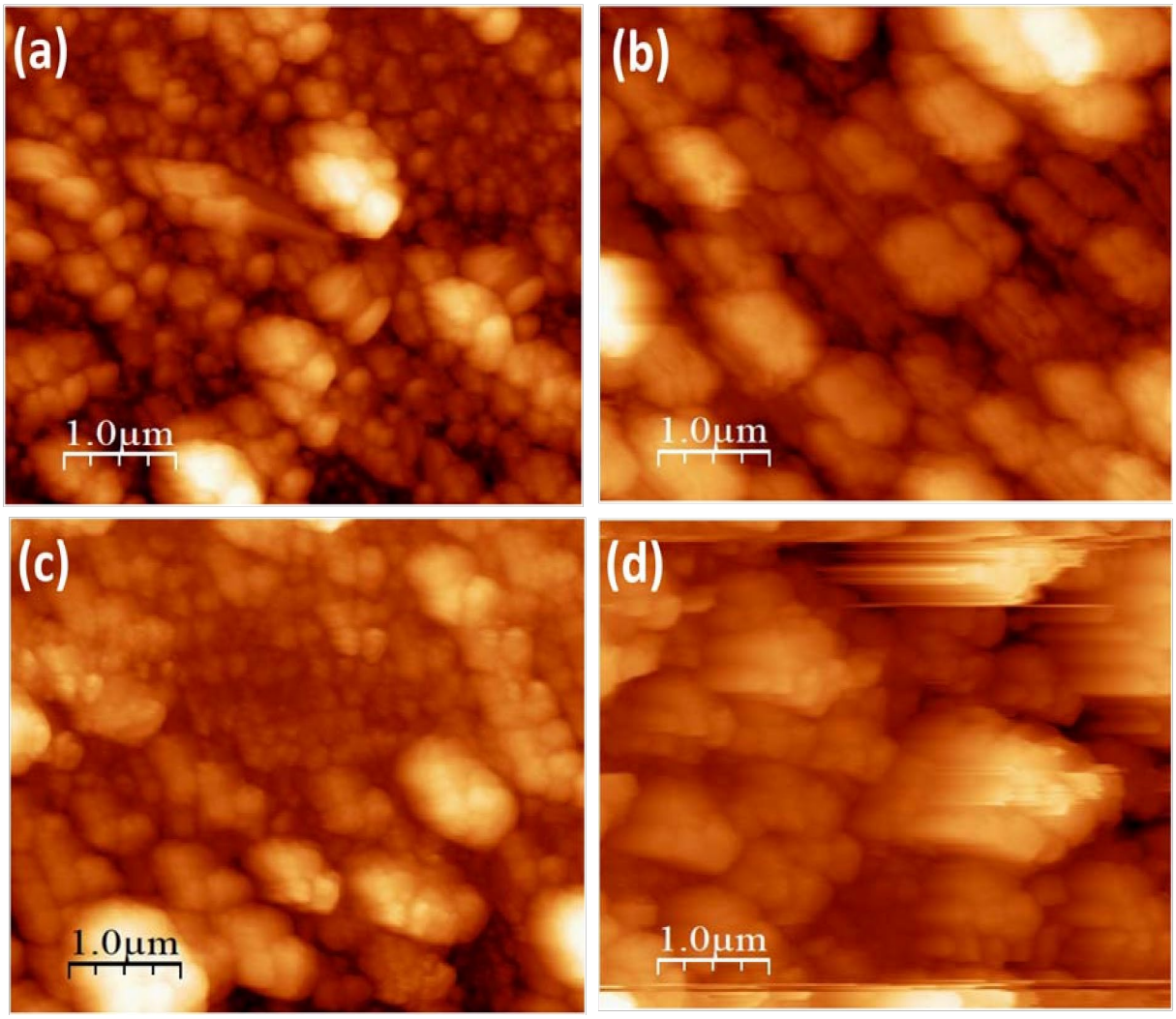

Fig. 8. AFM images of PbS nanostructures for varying film deposition time (a) 20 min, (b) 30 min, (c) 40 min, and (d) 50 min

Table 4. Value of grain size and root mean square (RMS) roughness of the different nanocrystalline PbS thin films

Deposition time (min)	20	30	40	50
Surface Roughness (nm)	104	120	132	256
Particle size (nm)	326	352	410	430

3.5. Optical Study

To understand the optical behavior of prepared nanocrystalline PbS thin films the transmission and absorption measurements were carried out by UV-Vis spectrophotometer. The measurements of transmission and absorption of nanocrystalline PbS thin films deposited by varying the deposition time were recorded in the range of 500 to 1000 nm. The nanocrystalline PbS thin films were dark brown in color and the optical transmittance of the film synthesized at 20 min deposition time was nearly 13% at a wavelength of 1000 nm. From Fig.9, it is found that the transmittance of the films is decreased from 13% to 7% when the deposition time increased from 20 min to 40 min. On further increasing the deposition time to 50 min, the transmittance of the film was found to be increased. Low value of transmittance might be attributed to the larger thickness of the nanocrystalline PbS thin films, while variation in the optical transmittance might be related to the variation in crystallite size with respect to the deposition time as evident from the XRD studies. Inset of Fig. 9 shows the absorbance of nanocrystalline PbS thin films prepared by varying the deposition time.

This figure shows that all samples have good absorbance in the visible region and low absorbance in near-infrared regions. These results suggest that the prepared material to be useful in several solar energy harvesting devices. From this Fig. it is observed that absorbance has higher value for the nanocrystalline PbS thin films deposited for 40 minute of deposition time. This indicates that optical properties of chemically deposited nanocrystalline PbS thin films are strongly influenced by the deposition parameter like deposition time.

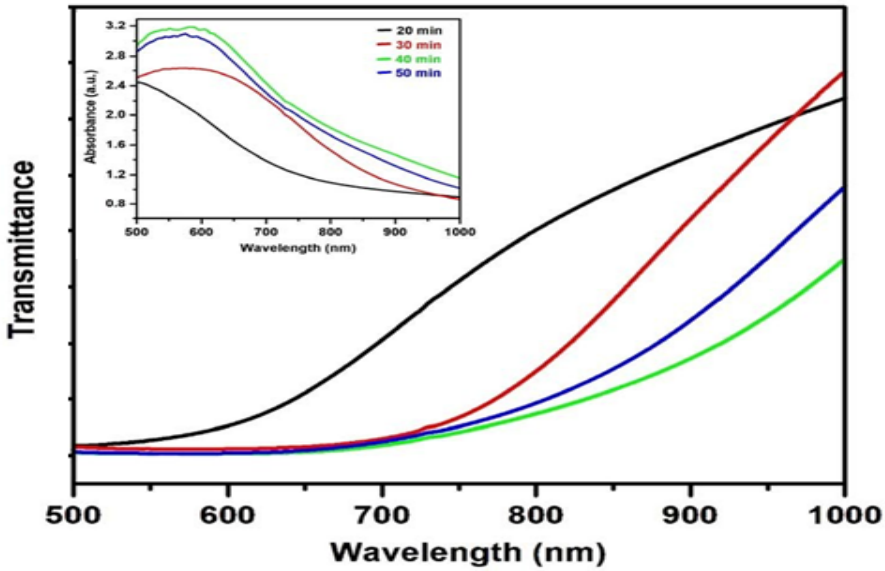

Fig. 9. Transmittance of nanocrystalline PbS thin films deposited on glass substrate at different deposition times. The inset shows the absorbance spectra obtained for the same thin films.

The value of the optical bandgap energy (E_g) of nanocrystalline PbS thin films is calculated by extrapolating the linear region of $(\alpha h\nu)^2$ versus $h\nu$ plot. Fig. 10 in inset shows typical plot of $(\alpha h\nu)^2$ versus $h\nu$ for nanocrystalline PbS thin films deposited at 20 min while Fig. 10 shows variation of energy bandgap as a function of deposition time. The calculated band gap energy values vary slightly; i.e. 1.75 eV, 1.5 eV, 1.48 eV, and 1.59 eV for the deposition times of 20 min, 30 min, 40 min, and 50 min, respectively [8].

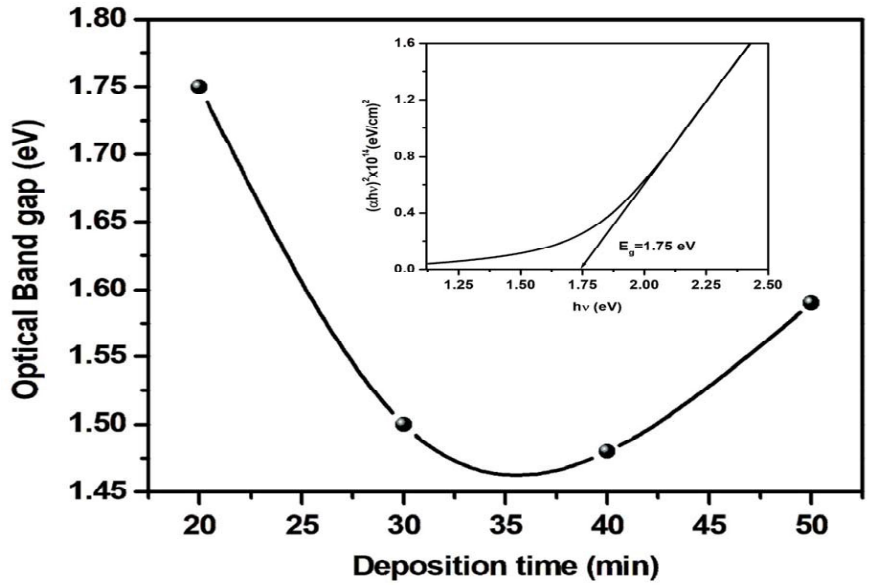

Fig. 10. Optical band gap versus deposition time of PbS thin films. The inset shows plot of $(\alpha h\nu)^2$ with respect to $h\nu$ (eV) for nanocrystalline PbS thin films deposited in 20 min.

This variation in the energy band gap can be due to higher contributions received from the electronic, ionic, dipolar, and space charge polarizations of charges [9]. This molecular orientation arises from gathering of a greater number of molecules having electric dipole which can be changed upon its orientation when an electrical or optical field is applied. The small-sized particles may necessitate large number of particles per unit volume i.e aspect ratio, resulting in an increase of the electrical charge dipole per unit volume, and variations in energy band gap and electrical conductivity could results [37].

3.6. Electrical Resistivity Measurement

Conventional two-point probe technique was used to measure the dark resistance at room temperature using pico-ammeter and voltmeter. Current-voltage behavior of chemically prepared nanocrystalline PbS thin films in dark current situation is shown in Fig. 11.

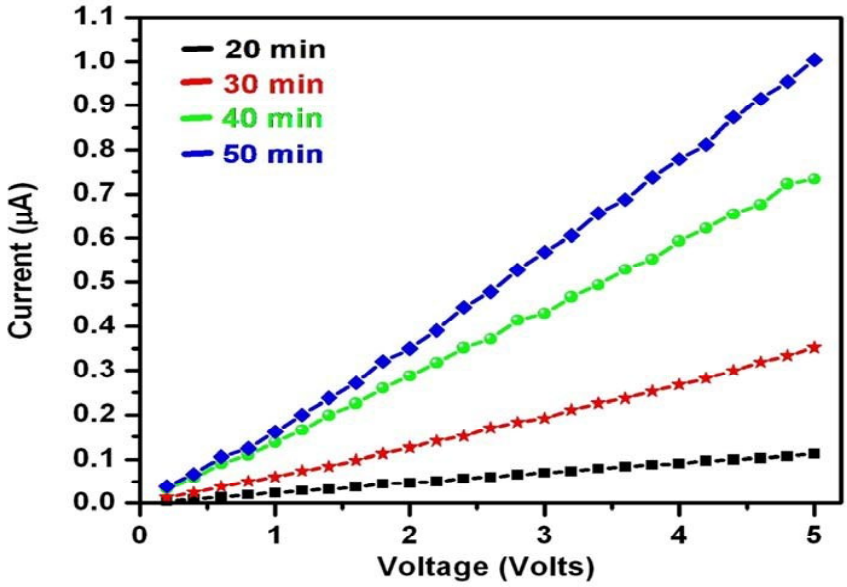

Fig. 11. Current voltage (I-V) characteristics of nanocrystalline PbS thin films prepared at different deposition time 20, 30, 40, and 50 min

It was observed from all I-V plots that there is no rectification behavior in thin films confirms that silver (Ag) makes ohmic contact with the synthesized PbS semiconductor [16]. This is the reason why we have shown only positive voltages for all PbS thin films. Also as seen from Fig. 11 that there is a significant effect of deposition time on the dark current, i.e., resistance of the deposited films. It shows that the dark current of thin films increases by increasing the deposition time [35].

This finding shows that band structure modification, quantum confinement effect, and increase in crystallite arrangement leads to better carrier transport in thin films [8, 17]. Fig. 12 shows the dependence of the electrical resistivity of the nanocrystalline PbS thin films on deposition time. As seen, the electrical resistivity of the films exponentially decreases from 69.4 MΩ.cm to 7.65 MΩ.cm with increasing deposition time.

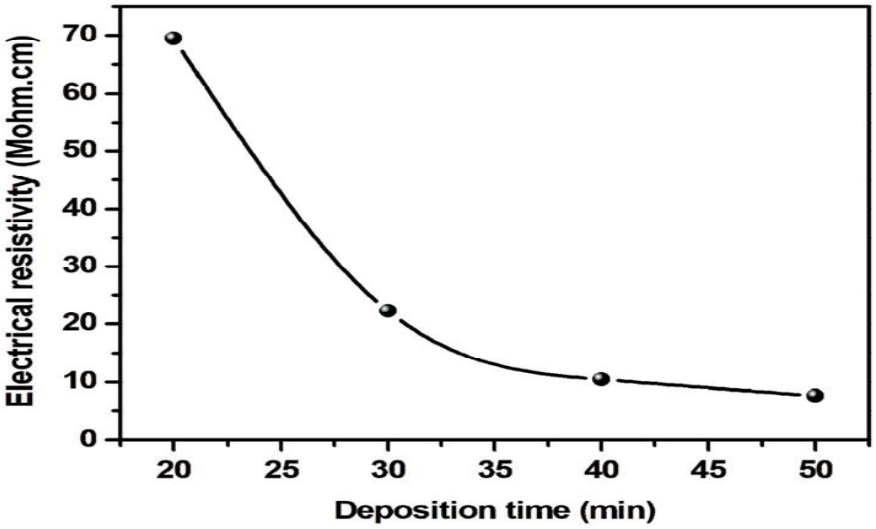

Fig. 12. Electrical resistivity versus deposition time of nanocrystalline PbS thin films

3.7. Ammonia Gas Sensing

Ammonia gas detection testing was conducted for PbS thin films at room temperature using the optical absorbance method. PbS thin film inserted vertically in the gas chamber and change in optical absorbance of the thin film detected. It is observed that absorbance of the film increases when ammonia is purged in the chamber, indicating the adsorption and surface reaction occurred between ammonia and PbS. The change in absorbance of sensor is shown in Fig. 13.

The sensitivity of the sensor is defined by using (standard) relation, $S = (A_g - A_a)/A_a$ where A_g and A_a are the

absorptions of films in gas and in air, respectively. These absorbance values are measured at 800 nm wavelength only. Fig. 13 shows the change in sensitivity of optical gas sensor with respect to thin film deposited at different dipping times. The sensitivity of the sensor increases with increase in dipping time, i.e., for thin film prepared using 40 min deposition time shows peak value of 85% sensitivity while for 50min dipping time it decreases to 70%. This variation can be correlated to surface morphology and composition dependent chemisorption process of the material. The thin film deposited at 40min time duration might have been stoichiometric which resulted into obtaining of particular results whereas films for least time durations like 20 and 30min might not have been saturated and thereby the sensitivity observed to be comparatively lower.

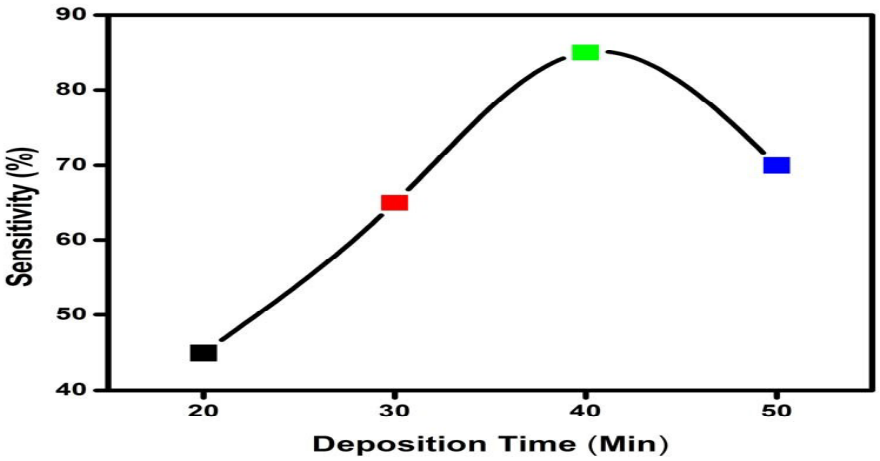

Fig. 13. Plot of PbS thin films deposition time against the sensitivity

Conclusions

From the above study it can be concluded that the stoichiometric PbS thin films can be successfully grown over the glass substrate using cost effective chemical route at room temperature. Stoichiometry can be achieved for the thin film dipping time of 40min. The characterizations and result obtained represented that the structural properties of PbS thin films revealed orientation along (111) and (002) planes with crystallite size varying from 18 to 22 nm. The Raman spectrum shows expected peaks as a combination of longitudinal and transverse acoustic (LA+TA) phonon modes in PbS thin films. The beauty of the PbS thin films can be clearly seen in the morphology of the materials as observed from the FESEM imaging, that is, the floral appearance with clear distinctions of petals like structure. The optical properties have revealed that PbS thin film deposited for 40min duration possesses the higher optical absorbance coefficient, energy band gap at 1.48 eV. As seen, the electrical resistivity of the films exponentially decreases from 69.4 MΩ.cm to 7.65 MΩ.cm with increasing deposition time. The gas sensing response confirmed that the film deposited for 40 min shows high sensitivity of 80% for ammonia gas compared to other films deposited at different time intervals.

Funding Statement

This research received no specific grant from any funding agency.

Conflicts of Interest

The authors declare no conflicts of interest.

Authors' Contributions

All authors contributed equally to this work.

References

[1] Hussain, A., Begum, A. and Rahman, A., 2013. Characterization of nanocrystalline lead sulphide thin films prepared by chemical bath deposition technique. *Arabian Journal for Science and Engineering*, *38*, pp.169-174.

[2] Slonopas, A., Alijabbari, N., Saltonstall, C., Globus, T. and Norris, P., 2015. Chemically deposited nanocrystalline lead sulfide thin films with tunable properties for use in photovoltaics. *Electrochimica Acta*, *151*, pp.140-149.

[3] Contreras-Rascón, J.I., Díaz-Reyes, J., Luna-Suárez, S., Carrillo-Torres, R.C. and Sánchez-Zeferino, R., 2019. Characterisation of chemical bath deposition PbS nanofilms using polyethyleneimine, triethanolamine and ammonium nitrate as complexing agents. *Thin Solid Films*, *692*, p.137609.

[4] Hone, F.G. and Dejene, F.B., 2018. Synthesis and characterization of lead sulphide thin films from ethanolamine (ETA) complexing agent chemical bath. *Materials Research Express*, *5*(2), p.026409.

[5] Yücel, Y. and Yücel, E., 2018. Synthesis and characterization of lead sulfide thin films by coumarin assisted CBD method. *Optik*, *164*, pp.263-270.

[6] Thirumavalavan, S., Mani, K. and Suresh, S., 2015. Investigation on structural, optical, morphological and electrical properties of lead sulphide (PbS) thin films. *Journal of Ovonic Research*, *11*(3), pp.123-130.

[7] Suresh, S. and Arunseshan, C., 2014. Dielectric properties of cadmium selenide (CdSe) nanoparticles synthesized by solvothermal method. *Applied Nanoscience*, *4*, pp.179-184.

[8] da Silva Filho, J.M.C. and Marques, F.C., 2019. Structural and optical temperature-dependent properties of PbS thin films deposited by radio frequency sputtering. *Materials Science in Semiconductor Processing*, *91*, pp.188-193.

[9] Preobrajenski, A.B. and Chassé, T., 1999. Epitaxial growth and interface structure of PbS on InP (110). *Applied surface science*, *142*(1-4), pp.394-399.

[10] Motlagh, Z.A. and Araghi, M.E.A., 2015. Effect of annealing temperature on optical and electrical properties of lead sulfide thin films. *Materials Science in Semiconductor Processing*, *40*, pp.701-707.

[11] Chaudhary, A., Klebanov, M. and Abdulhalim, I., 2015. PbS nanosculptured thin film for phase retarder, anti-reflective, excellent absorber, polarizer and sensor applications. *Nanotechnology*, *26*(46), p.465703.

[12] Singh, B.P., Kumar, R., Kumar, A. and Tyagi, R.C., 2015. Vacuum deposition of stoichiometric crystalline PbS films: the effect of sulfurizing environment during deposition. *Materials Research Express*, *2*(10), p.106401.

[13] Cheraghizade, M., Jamali-Sheini, F. and Yousefi, R., 2017. Optical, electrical, and photovoltaic properties of PbS thin films by anionic and cationic dopants. *Applied Physics A*, *123*(6), p.390.

[14] Akhtar, J., Afzaal, M., Vincent, M.A., Burton, N.A., Hillier, I.H. and O'Brien, P., 2011. Low temperature CVD growth of PbS films on plastic substrates. Chemical Communications, 47(7), pp.1991-1993.

[15] Yang, Y.J., 2006. A novel electrochemical preparation of PbS nanoparticles. *Materials Science and Engineering: B*, *131*(1-3), pp.200-202.

[16] Vankhade, D. and Chaudhuri, T.K., 2019. Effect of thickness on structural and optical properties of spin-coated nanocrystalline PbS thin films. *Optical Materials*, *98*, p.109491.

[17] Sarica, E. and Bilgin, V., 2017. Effect of Pb: S molar ratio in precursor solution on the properties of lead sulphide thin films by ultrasonic spray pyrolysis. *Materials Science in Semiconductor Processing*, *71*, pp.42-49.

[18] Veena, E., Bangera, K.V. and Shivakumar, G.K., 2016. Effect of substrate temperature on the structural and electrical properties of spray deposited lead sulfide thin films. *Materials Today: Proceedings*, *3*(6), pp.2225-2231.

[19] RaviShankar, S., Balu, A.R., Anbarasi, M. and Nagarethinam, V.S., 2015. Influence of precursor molar concentration on the structural, morphological, optical and electrical properties of PbS thin films deposited by spray pyrolysis technique using perfume atomizer. *Optik*, *126*(20), pp.2550-2555.

[20] Murza, V., Friedman, O., Vradman, L. and Golan, Y., 2018. Liquid flow deposition of PbS films on GaAs (100). *CrystEngComm*, *20*(26), pp.3765-3771.

[21] Obaid, A.S., Mahdi, M.A., Yusof, Y., Bououdina, M. and Hassan, Z., 2013. Structural and optical properties of nanocrystalline lead sulfide thin films prepared by microwave-assisted chemical bath deposition. *Materials science in semiconductor processing*, *16*(3), pp.971-979.

[22] Yücel, E., Yücel, Y. and Beleli, B., 2015. Process optimization of deposition conditions of PbS thin films grown by a successive ionic layer adsorption and reaction (SILAR) method using response surface methodology. *Journal of Crystal Growth*, *422*, pp.1-7.

[23] Preetha, K.C., Murali, K.V., Ragina, A.J., Deepa, K., Dhanya, A.C. and Remadevi, T.L., 2013, May. The role of cationic precursors in structural, morphological and optical properties of PbS thin films. In *IOP Conference Series: Materials Science and Engineering* (Vol. 43, No. 1, p. 012009). IOP Publishing.

[24] Baruah, B.J. and Sarma, K.C., 2017. Remarkable change of structural, optical, photoluminescence and electrical properties of chemically prepared nanocrystalline films of PbS with concentration of triethanolamine (TEA). *Journal of Materials Science: Materials in Electronics*, *28*, pp.5913-5924.

[25] Choudhury, N., 2016. Chemically deposited nanocrystalline PbS: effect of substrates. Indian Journal of Physics, 90(3), pp.283-287.

[26] Choudhury, N. and Sarma, B.K., 2011. Structural analysis of chemically deposited nanocrystalline PbS films. *Thin Solid Films*, *519*(7), pp.2132-2134.

[27] Choi, C.H., Paul, B.K. and Chang, C.H., 2014. Microreactor-assisted solution deposition for compound semiconductor thin films. *Processes*, *2*(2), pp.441-465.

[28] Gosavi, S.R., Nikam, C.P., Shelke, A.R., Patil, A.M., Ryu, S.W., Bhat, J.S. and Deshpande, N.G., 2015. Chemical synthesis of porous web-structured CdS thin films for photosensor applications. *Materials Chemistry and Physics*, *160*, pp.244-250.

[29] Seghaier, S., Kamoun, N., Brini, R. and Amara, A.B., 2006. Structural and optical properties of PbS thin films deposited by chemical bath deposition. *Materials Chemistry and Physics*, *97*(1), pp.71-80.

[30] Chattarki, A.N., Kamble, S.S. and Deshmukh, L.P., 2012. Role of pH in aqueous alkaline chemical bath deposition of lead sulfide thin films. *Materials Letters*, *67*(1), pp.39-41.

[31] Sonavane, D.K., Jare, S.K., Kathare, R.V., Bulakhe, R.N. and Shim, J.J., 2018. Chemical synthesis of PbS thin films and its physicochemical properties. Materials Today: Proceedings, 5(2), pp.7743-7747.

[32] Puspitasari, I., Gujar, T.P., Jung, K.D. and Joo, O.S., 2007. Simple chemical preparation of CuS nanowhiskers. Materials Science and Engineering: B, 140(3), pp.199-202.

[33] Hone, F.G. and Dejene, F.B., 2017. Tuning the optical band gap and stoichiometric ratio of chemically synthesized lead selenide thin films by controlling film thickness. *Journal of Materials Science: Materials in Electronics*, *28*, pp.5979-5989.

[34] Ovsyannikov, S.V., Shchennikov, V.V., Cantarero, A., Cros, A. and Titov, A.N., 2007. Raman spectra of (PbS) 1.18 (TiS2) 2 misfit compound. Materials Science and Engineering: A, 462(1-2), pp.422-426.

[35] Horcas, I., Fernández, R., Gomez-Rodriguez, J.M., Colchero, J.W.S.X., Gómez-Herrero, J.W.S.X.M. and Baro, A.M., 2007. WSXM: A software for scanning probe microscopy and a tool for nanotechnology. Review of scientific instruments, 78(1).

[36] Koaib, J., Bouguila, N., Abassi, H., Moutia, N., Kraini, M., Timoumi, A., Vázquez-Vázquez, C., Khirouni, K. and Alaya, S., 2020. Dielectric and electrical properties of annealed ZnS thin films. The appearance of the OLPT conduction mechanism in chalcogenides. *RSC advances*, *10*(16), pp.9549-9562.

[37] Baruah, B.J., Bora, M.N., Saikia, L., Saikia, D., Phukan, P. and Sarma, K.C., 2016. Effects of deposition temperature on structural, optical and electrical properties of TEA complexed nanocrystalline films of PbS prepared from lead acetate with reduced concentration. *Journal of Materials Science: Materials in Electronics*, *27*, pp.3911-3917.